EFDA–JET–CP(14)01/32

A. Baron-Wiechec, A. Widdowson, E. Alves, C.F. Ayres, N.P. Barradas, S. Brezinsek, J.P. Coad, N. Catarino, K. Heinola, J. Likonen, G.F. Matthews, M. Mayer, P. Petersson, M. Rubel, W. van Renterghem, I. Uytdenhouwen and JET EFDA contributors

Global Erosion and Deposition Patterns in JET with the ITER-Like Wall

Global Erosion and Deposition Patterns in JET with the ITER-Like Wall

A. Baron-Wiechec[1], A. Widdowson[1], E. Alves[2], C.F. Ayres[1], N.P. Barradas[3], S. Brezinsek[4], J.P. Coad[1], N. Catarino2, K. Heinola[6], J. Likonen[5], G.F. Matthews[1], M. Mayer[7], P. Petersson[8], M. Rubel[8], W. van Renterghem[9], I. Uytdenhouwen[9] and JET EFDA contributors*

JET-EFDA, Culham Science Centre, OX14 3DB, Abingdon, UK

[1]EURATOM-CCFE Fusion Association, Culham Science Centre, OX14 3DB, Abingdon, OXON, UK
[2]Instituto Superior Técnico, Instituto de Plasmas e Fusão Nuclear, Universidade de Lisboa, Lisboa, Portugal
[3]Centro de Ciências e Tecnologias Nucleares, Instituto Superior Técnico,Universidade de Lisboa, Portugal
4Association EURATOM-Forschungszentrum Jülich, IPP, D-52425, Jülich, Germany
5Association EURATOM-TEKES, VTT, PO Box 1000, 02044 VTT, Espoo, Finland
6Association EURATOM-TEKES, University of Helsinki, PO Box 64, 00014 University of Helsinki, Finland
7Max-Planck-Institut für Plasmaphysik, 85748 Garching, Germany
8Royal Institute of Technology, Association, EURATOM-VR, 100 44 Stockholm, Sweden
9 SCK•CEN, the Belgian Nuclear Research cCentre, Boeretang 200, 2400 Mol, Belgium
** See annex of F. Romanelli et al, "Overview of JET Results", (24th IAEA Fusion Energy Conference, San Diego, USA (2012)).*

Preprint of Paper to be submitted for publication in Proceedings of the
21st International Conference on Plasma Surface Interactions, Kanazawa, Japan
26th May 2014 - 30th May 2014

ABSTRACT

A set of Be and W tiles removed after the ITER-like Wall campaigns (JET-ILW) 2011-2 have been profiled, and results indicate that the primary erosion site is in the main chamber (Be) as in previous carbon campaigns (JET-C). In particular the limiters tiles near the mid-plane are eroded and occurred predominantly during the limiter phases of discharges. Moreover, correlation between erosion from the inner wall cladding tiles and the Be deposition in the divertor has been observed. W is found at low concentrations on all plasma-facing surfaces of the vessel indicating deposition via plasma transport from initially the W divertor and from main chamber W-coated tiles, there are also traces of Mo (used as an interlayer for these coatings). Deposited films in the inner divertor have a layered structure, and every layer is dominated by Be with some W and O content.

1. INTRODUCTION

Plasma wall interactions create some of the greatest challenges for realisation of a fusion reactor. This is also true for ITER where tritium trapping due to implantation and co-deposition or plasma pollution due to impurities migrating from PFCs to the plasma are major concerns. After over two decades of JET operation with a carbon wall, the ITER-like wall project at JET (JET-ILW) was initiated to explore plasma performance and plasma-wall interaction processes with a full metal wall: bulk beryllium (Be) or Be-coated Inconel in the main chamber and bulk tungsten (W) or W-coated carbon fibre composites (CFC) in the divertor [1, 2]. The first period of operation after installation of the new wall ran from September 2011 to July 2012 [3, 4]. An extensive post-mortem surface analysis program has been carried out after the ILW campaign and initial results were published elsewhere and presented during the PFMC 2013 conference [5, 6, 7]. In this paper a more complete accounting of erosion and deposition regions is presented, with data from fifteen locations in the JET chamber cross-section as indicated in Fig.1, and more detailed information is also now available on the nature of the divertor deposition.

2. EXPERIMENTAL

Be marker tiles at poloidal locations in the main JET chamber and W coated CFC marker tiles in the divertor have been installed as shown in Figure 1: the tiles have an interlayer of Ni or Mo respectively as described in [3, 9]. The tiles were analysed prior to installation and after removal from the vessel by a set of ion beam analytical methods to determine the extent of erosion/ deposition. Ion beam analyses were carried out using a Van de Graaff accelerator at the IST/ITN in Lisbon. Three complementary techniques were used: nuclear reaction analysis (NRA), Rutherford Backscattering Spectrometry (RBS) and Particle Induced X-ray Emission (PIXE). NRA employed the $^{9}Be(^{3}He,p)^{11}Be$, $^{12}C(^{3}He,p)^{14}N$ and $^{2}H(^{3}He,p)^{4}He$ reactions for detection of Be, C and ^{2}H (or D, deuterium) respectively using a 2.3 MeV He^{3} beam at normal incidence, with the detector positioned at 135° to the direction of the incident beam. The chemical composition and thicknesses of the deposited layers were also analysed by RBS and PIXE using a 2.3 MeV protons at a scattering angle

of 150°. The analysed area (beam spot diameter) was ~1 mm. The experimental cross-sections for backscattering of protons from Be and ^{3}He nuclear reactions were obtained experimentally for the experimental geometry since experimental data are only available at scattering angles of 158.7° and 170° for protons and 150° and 90° for ^{3}He NRA. A 140 μm-thick Al film was placed in front of the detector to stop elastically-scattered particles, thereby providing almost background-free detection. For quantitative analyses, the reaction yields were compared with D implanted in W reference samples containing $36 \pm 4 \cdot 10^{15}$ D atoms cm^{-2}. The accuracy of the reference sample was ~3%. More details of the methods can be found elsewhere [8]. Experimental data were analysed by using NDF [10] and/or SIMNRA [11] software to determine the chemical composition and thickness of deposits. IBA analysis is supported by extensive analysis of changes of surface profile of the selected marker tiles using a tile profiler. A detailed description of the profiler setup and the method of the measurement can be found in [6]. Cores cut from selected divertor tiles were examined by scanning electron microscopy (SEM) using a JEOL type 6310 SEM with Energy Dispersive Spectrometry (EDS) using Noran Instruments equipment. The applied voltage was 15 keV for Secondary Electron (SE) or Back-Scattered Secondary Electron (BSE) viewing and EDS.

3. RESULTS

In this section the migration pattern is summarised for key areas of the main chamber and divertor. The implications are discussed in the next section.

3.1 DEPOSITION PATTERN IN THE MAIN CHAMBER

3.1.1. Outer poloidal limiters 4D 3-14-23

The erosion/deposition at the outer poloidal limiters (OPL) tiles is illustrated by the analyses of tiles from rows 3 (4D3), 14 (4D14) and 23 (4D23) located as indicated (Fig. 1). Visual inspection of the OPL has been reported in [3, 6]. Representative RBS spectra from a tile near the midplane (4D14) are presented in Fig.2. It shows that at the centre of this tile 4D14 the marker has been eroded and only bulk Be remains (Fig.2, region a), profilometry indicate erosion of up to 30μm. IBA shows re-deposition of Be and Ni coating onto both left and right sides (eg RBS in Fig.2, region b). However, the right side of the tile is also characterised by some spalling of the coating, which limits the accuracy of the IBA analysis. Nevertheless based on IBA it can be concluded that where the coating remains it is a mixture of mainly Be with Ni and W. Between the eroded area and the ends of the tile are transition regions where the surface is virtually as the original marker layer (Fig. 2, region c). Secondly, there is no indication of erosion or local erosion and deposition on the 4D3, the marker coating is still intact. The tile is relatively clean, with some signs of deposition on the outer layer of the Be/Ni marker coating; mainly W and clear surface signals from Ni, Mo, Cr, Fe. Finally, there has been no visible interaction of the plasma with the tile 4D23, and certainly any profile changes were below the technique limit (±5μm).

Tiles B and C placed between outer divertor tiles and the main chamber (Fig 1) were also analysed by means of IBA. These CFC tiles were originally coated with approximately 10μm thick W prior

to installation. There is no measurable change in profile of either tile the (less than 3μm), and NRA shows Be deposition (if any) is close to the spectrum background, not exceeding $1 \cdot 10^{15}$ at/cm^2. NRA also shows D concentrations on the tiles of ~$1 \cdot 10^{17}$ at/cm^2; the shape of the D peak in the NRA spectra suggests relatively deep incorporation of D into the material [8].

3.1..2 Inner wall guard limiters (IWGL) 2XR 3-10-19

Visual inspection of the IWGL from rows: 3 (2XR3), 10 (2XR10) and 19 (2XR19) located as indicated (Fig. 1) has been reported in [3, 6]. Surface profiler and IBA analysis of Be/Ni marker tiles 2XR3, 2XR10 and 2XR19 has been completed recently. At the centre of tile 2XR10 the marker has vanished and only bulk Be remains, and profilometry indicate erosion of up to 60 μm. Towards the sides of the tile there is deposition of some Be and plasma impurities such as W and Ni, Mo, Cr, Fe (identified by PIXE) typical for Inconel composition, and at the very edges the composition reverts to the original marker composition (similar to Fig.2, region c). The marker tracer at the centre part of the top limiter 2XR19 is intact/conserved so no erosion has occurred, whilst at the centre of 2XR3 there is some thinning of the Be marker. These observations confirm the preliminary estimated erosion rate from the mid-plane of IWGL, of approximately 2.3 x 10e19 atoms s^{-1} [3] which were based on a single tile. Analysis of 2XR3 indicates erosion with simultaneous deposition within the area of the central part of the tile and also a thick deposit (mainly Be with no more than 0.05% of W and 0.08% Ni) of thickness around 7-$10 \cdot 10^{18}$ at/cm^2 mostly on left side of the middle part and wing, Fig.4. IBA findings are in good agreement and are complementary to surface profilometry. Neither erosion nor significant deposition on the top of the inner limiter 2XR19 is observed, just traces of W and Ni.

3.1.3 Distribution of W and Ni on inner and outer limiters and dump plates (DP)

It is important to highlight the presence of W in the range 1 to $50 \cdot 10^{15}$ at/cm^2 and Ni in the range less than 4 to $40 \cdot 10^{15}$ at/cm^{2}on the surface of all analysed tiles from the main chamber. The amount of W, Ni and also traces of Fe, Cr, Ti or Mo were calculated by combining RBS and PIXE data. The combined amount of Mo, Cr and Fe does not exceed 0.1% of the elemental composition of the deposit. On the surface of the top IWGL (2XR19), the W surface peak signal (accompanied by Ni surface signal, not related to the underlying marker) is greater on the right side of the limiter, whereas in the case of the middle tile 2XR10 and lower tile 2XR3, the W concentration is higher on the left side of the tile – this is consistent with the pattern of deposition on the IWGL that was observed throughout the JET-C campaign. At the time of writing the manuscript only two OPL tiles were analysed by means of IBA, namely 4D3 and 4D14. Tungsten and Nickel have been found on both tiles, with a higher concentration on left side of the tiles; on the tile 4D14 the W concentration on the right side was negligible (below $5 \cdot 10^{15}$ at/cm^2). Extensive melting along the poloidal ridge of the dump plate (DP) was found at all locations around the top of the machine and appears toroidally uniform in character. The melted ridge is closest to the plasma. Traces of W

in the range from 5 to 40 $\cdot 10^{15}$ at/cm^2 and Ni in the range from 20 to 50 $\cdot 10^{15}$ at/cm^2 were found on the DP surface, with a higher content of W impurities on the side where arc tracks are visible. Based on profiler measurements the net erosion of the DP tiles is approximately zero ± 5 μm (limit of the surface profiler accuracy).

3.2 DEPOSITION PATTERN IN DIVERTOR

The summary of the deposition and erosion zones in the divertor, including Be concentration and also C and O concentration where it was possible to calculate have been reported [3, 5, 7]. The composition of the deposit is mainly Be with traces of W, Ni, Mo, Cr and Fe. Only small amounts of Be have been found on Tile 3, 4, 6 and 7 (less that $1 \cdot 10^{18}$ at/cm^2), indeed SEM analysis suggest there may be some signs of erosion of lower part of Tile 1 and upper part of Tile 3. The thickest deposit has been found on top of Tile 1 (~15μm, two points where it might be more than 17 μm – the maximum accessible for IBA) and on the High Field Gap Closure (HFGC) tile (in the range from 3 to 8μm); there is no data from surface profilometry from these areas. RBS spectra of all the Be deposition, but particularly the thick deposit on tile 1 have proved difficult to fit with the WinDF or SIMNRA software. The surfaces are known to be rough, but it was not possible to say to what extent the problems were related to the surface roughness and/or chemical composition variability of the deposit. A fitting of the spectra by using sets of Be-W layers of slightly different Be to W ratio (ratio decreases towards the substrate) could give relatively good agreement with the measured spectra. However, it should be kept in mind that the data analysis assumes a flat surface. For the derived depth profiles roughness effects are interpreted as depth profiles of elements. Nevertheless, it has been already shown that in case of ambiguities between depth profiles and surface roughness the total amounts of elements are still correct even if the depth profiles may not reflect the sample structure correctly [12]. Recent scanning microscopy of a sample cross-section has brought some clarification for interpreting RBS spectra and confirmed a multi-layered structure of the thickest deposited material, which is clearly observed on tile 1, as shown in Fig.3a. Combining the information of the BSE microscopy, the EDS analysis and IBA, it can be concluded that the deposited material has a multi-layered structure consisting of an outer layer of pure Be and inner layer of mixed Be and W layers with W/Be ratio: 0.05–0.08 (Fig.3b). The oxygen concentration was not possible to evaluate in this work by IBA but it might be likely that the inner layer contains also a significant amount of oxygen (up to 10 %). The darker layers have a higher Be/W ratio, while the brighter layers contain more W. Due to the thinness of the layers, the EDS analysis could not be limited to a single layer and, therefore, it is not excluded that pure Be and W layers are deposited alternately, without mixing. The upper part of Tile 1, revealed areas of non-uniformity of the deposit (small cracks), Fig.3c; by contrast the vertical part of Tile 1, and Tiles 4 and 6 are characterised by a cauliflower-like morphology, as in Fig. 3d. The amount of material deposited on Tiles 4 and 6 was below ~$2.5 \cdot 10^{18}$ at/cm^2, but some deposition was found, mainly in the sloped part of tiles (~$6 \cdot 10^{18}$ at/cm^2 of Be). The thickness of the deposition is of the order of a hundred nanometres to 1μm, but

in the valleys between the fibres, the deposition thickness can increase up to 5 μm,. In the thickest part of the deposit it was again found that it is built up by a multi-layer structure of different intensity in the BSE image, indicating a different composition of the layers (Fig. 3e).

4. DISCUSSION AND CONCLUSION

The latest quantitative assessment of the overall migration balance based on a combination of surface profilometry and accelerator based ion beam techniques is summarised in Table 1. The results are consistent with the preliminary values [3] but are based on more quantitative data such as cross sections and analysis of inner wall cladding. The general picture painted based on marker analysis and surface profilometry is that the major erosion areas are the central tiles of the Be IWGLs, with a lesser erosion area at the centre of the OPL with the strong caveats that tiles from only a limited selection of poloidal locations were removed and with no check on toroidal uniformity other than the detailed visual examination of every tile in the vessel. The rate of erosion at the IWGL during the limiter phases of ILW operations has been calculated to be similar to that during the previous carbon campaign [3]. It is expected that erosion during the limiter phases will be balanced by re-deposition on limiter surfaces deeper into the scrape-off layer (SOL) but despite more measurements this balance has not been demonstrated due to the limited number of tile samples, surface roughness and/or spalling of coating in deposition areas [1, 2]. During the divertor phase of each discharge erosion is probably dominated by charge exchange neutral (CXN) bombardment of the main chamber wall and migration along the SOL to the inner divertor. This is evidenced by erosion measurements at the Inner Wall Cladding (IWC) tiles that line the vessel wall between the IWGL [13] which suggest that the IWC may account for a significant fraction of the Be deposition found in the divertor. Some contribution may also be expected from re-erosion of the deposits on the IWGL, which may have a higher erosion yield than the bulk material. Melting of Be tiles occurred at Dump Plate tiles and also at some castellation edges on IWGL tiles. Furthermore, there is W found on the surface of all tiles in the JET vessel, including tiles that were pure Be, and the amounts at the surface are of the same order of magnitude everywhere, from Dump Plates at the top of the vessel to divertor tiles at the bottom, and even to the louvre clips in shadowed areas. It seems unlikely that the divertor was the major source of the W. Furthermore, transient impurity events involving tungsten are relatively common [14]. It seems likely, therefore that the source of the W and Mo is from small particles of W coating (which has a Mo interlayer) coming off coatings in the main chamber; there are significant areas of W-coated CFC in the main chamber as well as in the divertor, such as wall protection in neutral beam shine-through areas, mushroom limiters at the top of the vessel and diagnostic protection covers. There are also many areas where widespread arcing has occurred that are visible on Be tiles: such arcing may also be widespread on W-coated CFC tiles but would not be easily visible, however could readily dislodge coating asperities from these rough surfaces. Deposition at the inner divertor is concentrated on the HFGC tiles and the inboard parts of tile 1. This pattern is more restricted than during the previous JET carbon campaigns, when deposition extended over all

tile 1 and also on tile 3. This may be partly due to the more limited range of plasma shapes employed during the ILW operations. However, the largest difference is probably the lack of strong chemical sputtering which both allowed low energy neutrals to efficiently sputter the carbon main chamber walls during the divertor phase and enabled long range migration within the divertor.

ACKNOWLEDGEMENT

This work was partly funded by the RCUK Energy Programme [grant number EP/I501045] and by the European Union Horizon 2020 research and innovation programme. The work was also part-funded by the European Communities under the contract of Association between EURATOM/CCFE within the framework of the European Fusion Development Agreement. The views and opinions expressed herein do not necessarily reflect those of the European Commission.

REFERENCES

[1]. G F Matthews et al., Physica Scripta (2011) 014001
[2]. C. Giroud et al., Nuclear Fusion **53** (2013) 113025
[3]. A Widdowson et al., 2014 Physica Scripta **T159** (2014) 014010
[4]. G.F. Matthews, Journal of Nuclear Materials **438** (2013) S2–S10,
[5]. J Likonen et al., 2014 Physica Scripta **T159** (2014) 014016,
[6]. K Heinola et al., Physica Scripta **T159** (2014) 014013,
[7]. J P Coad et al., 2014 Physica Scripta **T159** (2014) 014012
[8]. K.Heinola et al., Physica Scripta **T128** (2007) 91-95
[9]. K.Heinola et al., this conference
[10]. N.P. Barradas, C. Jeynes, Nuclear Instruments and Methods in Physics Research Section B **266** (2008) 1875
[11]. M. Mayer, SIMNRA User‘s Guide, Report IPP 9/113, Max-Planck-Institut für Plasmaphysik, Garching, Germany, 1997
[12]. M. Mayer, W. Eckstein, H. Langhuth, F. Schiettekatte, U. von Toussaint, Nucl. Instr. Meth. B **269** (2011) 3006
[13]. S. Krat, Yu. Gasparyan, A. Pisarev, I. Bykov, M. Mayer, G. de Saint Aubin, M. Balden, C.P. Lungu, A. Widdowson, JET-EFDA contributors, Erosion at the inner wall of JET during the discharge campaign 2011-2012 in comparison with previous campaigns, submitted to J. Nucl. Mater.
[14]. M. Sertoli et al., this conference
[15]. M. Mayer, Journal of Nuclear Materials **438** (2013) S780–S783
[16]. J.P. Coad, J. Likonen et al., this conference

	JET-ILW (2011-2) includes this work [3,4]	JET-C (2007-9) [3]
Plasma time, hours Limiter/ Divertor	6/13	12/33
Dump Plates	“melting”	130g (-)
IWGL		
2XR19 (1 row)	0	0.8g (+)
2XR10 (1 row)	8g (-)	11g (-)
2XR3 (1 row)	0	N
IWC (all)	15g (-)[15]	129g (-)
OPL		
4D23 (1 row)	0	NM
4D14 (1 row)	5g (-)	3.1g (-)
4D3 (1 row)	0	N
Divertor:		
HFGC	5-10 (+)	30g (+) [16]
Tile 1	25g (+)	65g (+) [16]
Tile 3,4,6	<6g (+)	428g (+) [16]
Tile 7,8	<4g (+/-)	64g (-)
Dust	1 [3]	233

+ indicates deposition, - indicates erosion,

Table 1: Quantitative assessment of the overall migration balance, net erosion/deposition.

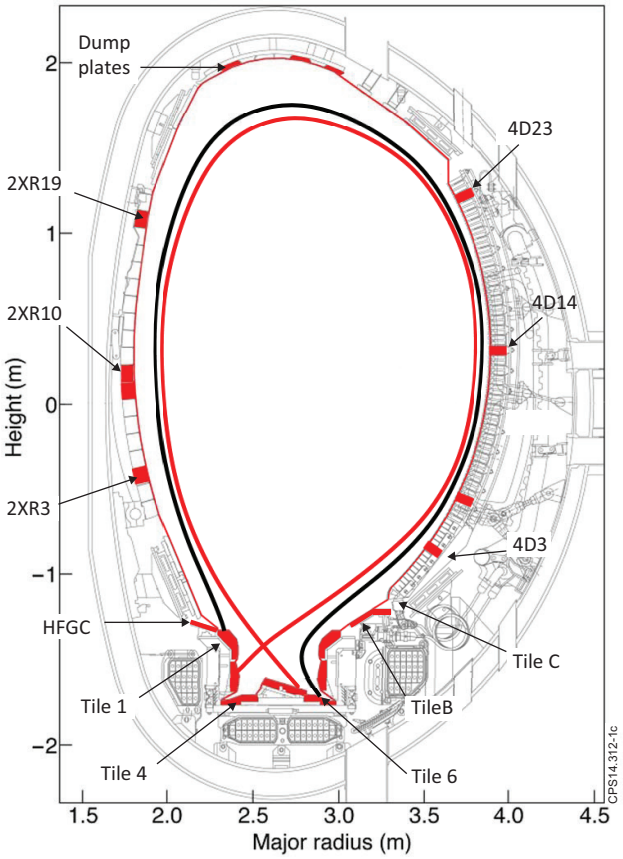

Figure 1: Poloidal cross-section of the JET vessel with investigated tiles location indicated.

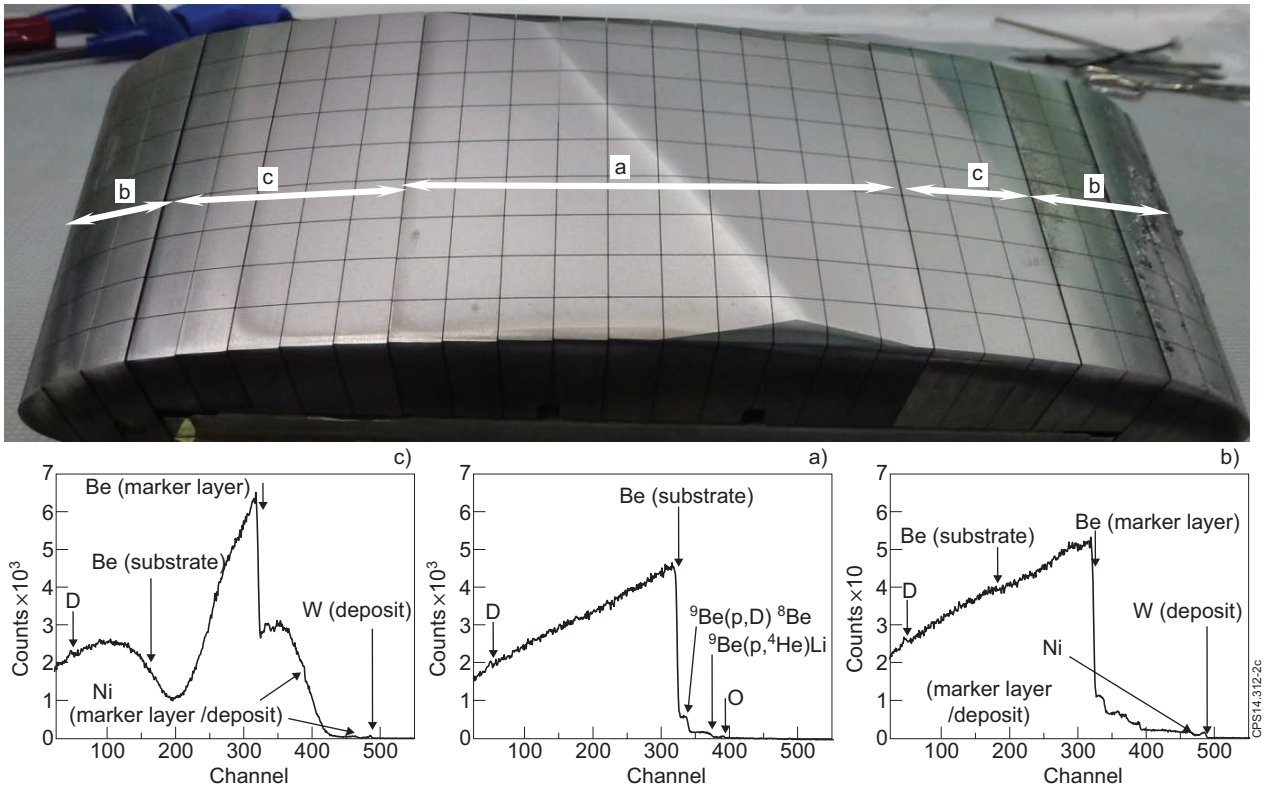

Figure 2: Photo of OPL (4D14) after ILW campaigns 2011-2 and the marker coating evaluation. RBS spectra of a central erosion zone (indicated by a), a left and right wing, deposition zone (indicated by b), and a middle part where the marker starts appearing (indicated by c).

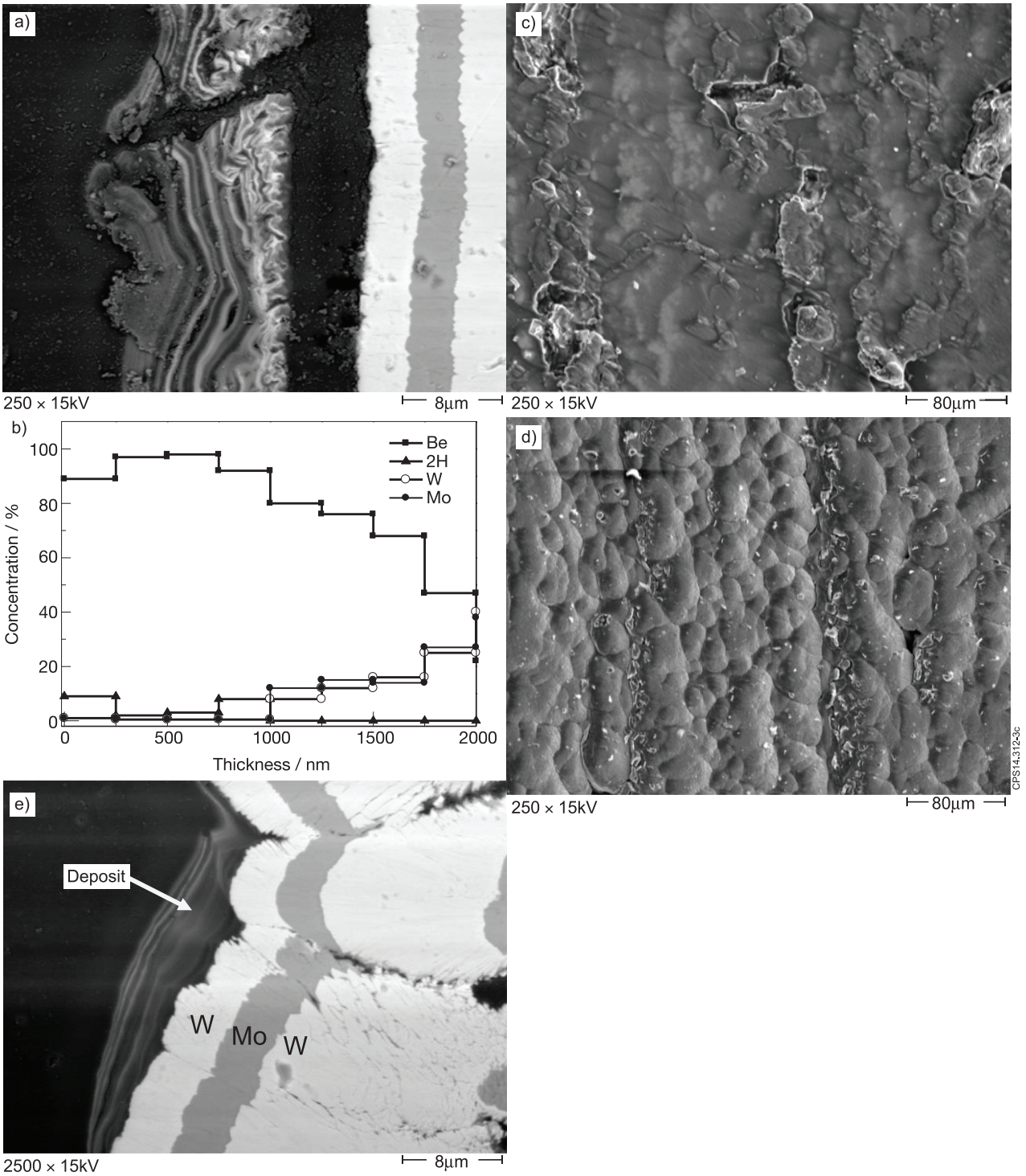

Figure 3: BSE image of a cross-section of the top part (apron) of tile 1, there is an open space marked by (1) between the marker coating and flake filled with resin during an embedding of the samples (a), corresponding elements distribution within 15-20µm calculatyed by WinDF software based on RBS/NRA/PIXIE data (b), BSE image of a top view of the upron of the tile 1 surface (c), characteristic cauliflower morphology BSE image of a top view of the tile 4 surface, characteristic cauliflower morphology (d), BSE image of a cross-section of the sloped part of tile 4 near the strike point, deposit in the valleys (e).

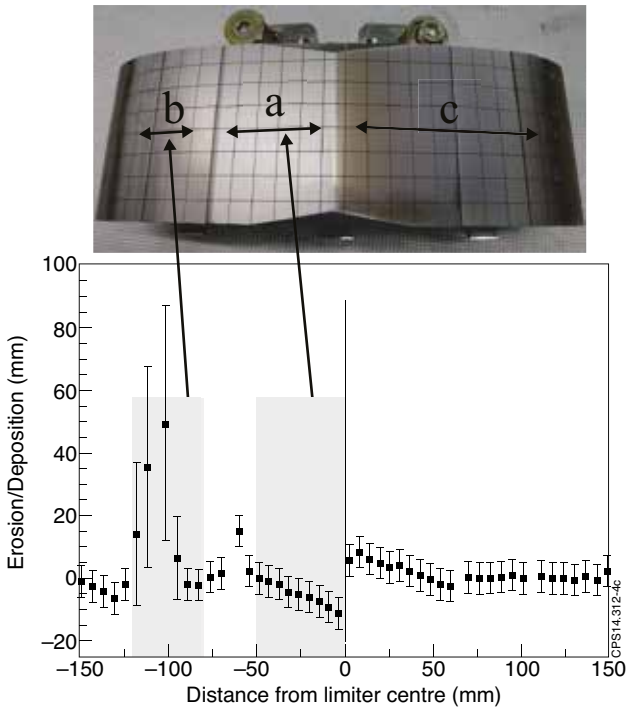

Figure 4: Surface profiling results for the IWGL beryllium tile (2XR3), the main deposition is observer on the left side of the wing tile and erosion on the left part of central tile, disappearance of Be marker confirmed by IBA: eroded Be marker (area a), deposition on top of the Be marker (area b), marker in tack/thinning of the marker (area c).